This paper is published as part of a *PCCP* themed issue series on biophysics and biophysical chemistry:

Biomolecular Structures: From Isolated Molecules to Living Cells

Guest Editors: Seong Keun Kim, Jean-Pierre Schermann and Taekjip Ha

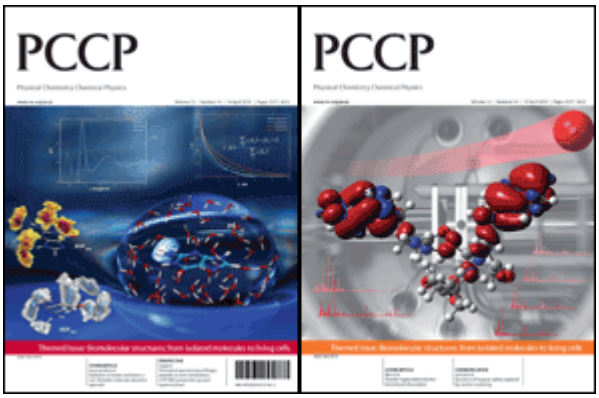

Editorial

Biomolecular Structures: From Isolated Molecules to the Cell Crowded Medium
Seong Keun Kim, Jean-Pierre Schermann, Taekjip Ha, *Phys. Chem. Chem. Phys.*, 2010
DOI: 10.1039/c004156b

Perspectives

Theoretical spectroscopy of floppy peptides at room temperature. A DFTMD perspective: gas and aqueous phase
Marie-Pierre Gaigeot, *Phys. Chem. Chem. Phys.*, 2010
DOI: 10.1039/b924048a

Communications

Dynamics of heparan sulfate explored by neutron scattering
Marion Jasnin, Lambert van Eijck, Michael Marek Koza, Judith Peters, Cédric Laguri, Hugues Lortat-Jacob and Giuseppe Zaccai, *Phys. Chem. Chem. Phys.*, 2010
DOI: 10.1039/b923878f

Papers

Infrared multiple photon dissociation spectroscopy of cationized methionine: effects of alkali-metal cation size on gas-phase conformation
Damon R. Carl, Theresa E. Cooper, Jos Oomens, Jeff D. Steill and P. B. Armentrout, *Phys. Chem. Chem. Phys.*, 2010
DOI: 10.1039/b919039b

Structure of the gas-phase glycine tripeptide
Dimitrios Toroz and Tanja van Mourik, *Phys. Chem. Chem. Phys.*, 2010
DOI: 10.1039/b921897a

Photodetachment of tryptophan anion: an optical probe of remote electron
Isabelle Compagnon, Abdul-Rahman Allouche, Franck Bertorelle, Rodolphe Antoine and Philippe Dugourd, *Phys. Chem. Chem. Phys.*, 2010
DOI: 10.1039/b922514p

A natural missing link between activated and downhill protein folding scenarios
Feng Liu, Caroline Maynard, Gregory Scott, Artem Melnykov, Kathleen B. Hall and Martin Gruebele, *Phys. Chem. Chem. Phys.*, 2010
DOI: 10.1039/b925033f

Vibrational signatures of metal-chelated monosaccharide epimers: gas-phase infrared spectroscopy of Rb^+-tagged glucuronic and iduronic acid
Emilio B. Cagmat, Jan Szczepanski, Wright L. Pearson, David H. Powell, John R. Eyler and Nick C. Polfer, *Phys. Chem. Chem. Phys.*, 2010
DOI: 10.1039/b924027f

Stepwise hydration and evaporation of adenosine monophosphate nucleotide anions: a multiscale theoretical study
F. Calvo and J. Douady, *Phys. Chem. Chem. Phys.*, 2010
DOI: 10.1039/b923972c

Reference MP2/CBS and CCSD(T) quantum-chemical calculations on stacked adenine dimers. Comparison with DFT-D, MP2.5, SCS(MI)-MP2, M06-2X, CBS(SCS-D) and force field descriptions
Claudio A. Morgado, Petr Jurečka, Daniel Svozil, Pavel Hobza and Jiří Šponer, *Phys. Chem. Chem. Phys.*, 2010
DOI: 10.1039/b924461a

Photoelectron spectroscopy of homogeneous nucleic acid base dimer anions
Yeon Jae Ko, Haopeng Wang, Rui Cao, Dunja Radisic, Soren N. Eustis, Sarah T. Stokes, Svetlana Lyapustina, Shan Xi Tian and Kit H. Bowen, *Phys. Chem. Chem. Phys.*, 2010
DOI: 10.1039/b924950h

Sugar–salt and sugar–salt–water complexes: structure and dynamics of glucose–KNO_3–$(H_2O)_n$
Madeleine Pincu, Brina Brauer, Robert Benny Gerber and Victoria Buch, *Phys. Chem. Chem. Phys.*, 2010
DOI: 10.1039/b925797g

Hydration of nucleic acid bases: a Car–Parrinello molecular dynamics approach
Alona Furmanchuk, Olexandr Isayev, Oleg V. Shishkin, Leonid Gorb and Jerzy Leszczynski, *Phys. Chem. Chem. Phys.*, 2010
DOI: 10.1039/b923930h

Conformations and vibrational spectra of a model tripeptide: change of secondary structure upon micro-solvation
Hui Zhu, Martine Blom, Isabel Compagnon, Anouk M. Rijs, Santanu Roy, Gert von Helden and Burkhard Schmidt, *Phys. Chem. Chem. Phys.*, 2010
DOI: 10.1039/b926413b

Peptide fragmentation by keV ion-induced dissociation
Sadia Bari, Ronnie Hoekstra and Thomas Schlathölter, *Phys. Chem. Chem. Phys.*, 2010
DOI: 10.1039/b924145k

Structural, energetic and dynamical properties of sodiated oligoglycines: relevance of a polarizable force field
David Semrouni, Gilles Ohanessian and Carine Clavaguéra, *Phys. Chem. Chem. Phys.*, 2010
DOI: 10.1039/b924317h

Studying the stoichiometries of membrane proteins by mass spectrometry: microbial rhodopsins and a potassium ion channel
Jan Hoffmann, Lubica Aslimovska, Christian Bamann, Clemens Glaubitz, Ernst Bamberg and Bernd Brutschy, *Phys. Chem. Chem. Phys.*, 2010
DOI: 10.1039/b924630d

Sub-microsecond photodissociation pathways of gas phase adenosine 5′-monophosphate nucleotide ions
G. Aravind, R. Antoine, B. Klærke, J. Lemoine, A. Racaud, D. B. Rahbek, J. Rajput, P. Dugourd and L. H. Andersen, *Phys. Chem. Chem. Phys.*, 2010
DOI: 10.1039/b921038e

DFT-MD and vibrational anharmonicities of a phosphorylated amino acid. Success and failure
Alvaro Cimas and Marie-Pierre Gaigeot, *Phys. Chem. Chem. Phys.*, 2010
DOI: 10.1039/b924025j

Infrared vibrational spectra as a structural probe of gaseous ions formed by caffeine and theophylline
Richard A. Marta, Ronghu Wu, Kris R. Eldridge, Jonathan K. Martens and Terry B. McMahon, *Phys. Chem. Chem. Phys.*, 2010
DOI: 10.1039/b921102k

Laser spectroscopic study on (dibenzo-24-crown-8-ether)–water and –methanol complexes in supersonic jets
Satoshi Kokubu, Ryoji Kusaka, Yoshiya Inokuchi, Takeharu Haino and Takayuki Ebata, *Phys. Chem. Chem. Phys.*, 2010
DOI: 10.1039/b924822f

Macromolecular crowding induces polypeptide compaction and decreases folding cooperativity
Douglas Tsao and Nikolay V. Dokholyan, *Phys. Chem. Chem. Phys.*, 2010
DOI: 10.1039/b924236h

Electronic coupling between cytosine bases in DNA single strands and *i*-motifs revealed from synchrotron radiation circular dichroism experiments
Anne I. S. Holm, Lisbeth M. Nielsen, Bern Kohler, Søren Vrønning Hoffmann and Steen Brøndsted Nielsen, *Phys. Chem. Chem. Phys.*, 2010
DOI: 10.1039/b924076d

Photoionization of 2-pyridone and 2-hydroxypyridine
J. C. Poully, J. P. Schermann, N. Nieuwjaer, F. Lecomte, G. Grégoire, C. Desfrançois, G. A. Garcia, L. Nahon, D. Nandi, L. Poisson and M. Hochlaf, *Phys. Chem. Chem. Phys.*, 2010
DOI: 10.1039/b923630a

Insulin dimer dissociation and unfolding revealed by amide I two-dimensional infrared spectroscopy
Ziad Ganim, Kevin C. Jones and Andrei Tokmakoff, *Phys. Chem. Chem. Phys.*, 2010
DOI: 10.1039/b923515a

Six conformers of neutral aspartic acid identified in the gas phase
M. Eugenia Sanz, Juan C. López and José L. Alonso, *Phys. Chem. Chem. Phys.*, 2010
DOI: 10.1039/b926520a

Binding a heparin derived disaccharide to defensin inspired peptides: insights to antimicrobial inhibition from gas-phase measurements
Bryan J. McCullough, Jason M. Kalapothakis, Wutharath Chin, Karen Taylor, David J. Clarke, Hayden Eastwood, Dominic Campopiano, Derek MacMillan, Julia Dorin and Perdita E. Barran, *Phys. Chem. Chem. Phys.*, 2010
DOI: 10.1039/b923784d

Guanine–aspartic acid interactions probed with IR–UV resonance spectroscopy
Bridgit O. Crews, Ali Abo-Riziq, Kristýna Pluháčková, Patrina Thompson, Glake Hill, Pavel Hobza and Mattanjah S. de Vries, *Phys. Chem. Chem. Phys.*, 2010
DOI: 10.1039/b925340h

Investigations of the water clusters of the protected amino acid Ac-Phe-OMe by applying IR/UV double resonance spectroscopy: microsolvation of the backbone
Holger Fricke, Kirsten Schwing, Andreas Gerlach, Claus Unterberg and Markus Gerhards, *Phys. Chem. Chem. Phys.*, 2010
DOI: 10.1039/c000424c

Probing the specific interactions and structures of gas-phase vancomycin antibiotics with cell-wall precursor through IRMPD spectroscopy
Jean Christophe Poully, Frédéric Lecomte, Nicolas Nieuwjaer, Bruno Manil, Jean Pierre Schermann, Charles Desfrançois, Florent Calvo and Gilles Grégoire, *Phys. Chem. Chem. Phys.*, 2010
DOI: 10.1039/b923787a

Two-dimensional network stability of nucleobases and amino acids on graphite under ambient conditions: adenine, L-serine and L-tyrosine
Ilko Bald, Sigrid Weigelt, Xiaojing Ma, Pengyang Xie, Ramesh Subramani, Mingdong Dong, Chen Wang, Wael Mamdouh, Jianguo Wang and Flemming Besenbacher, *Phys. Chem. Chem. Phys.*, 2010
DOI: 10.1039/b924098e

Importance of loop dynamics in the neocarzinostatin chromophore binding and release mechanisms
Bing Wang and Kenneth M. Merz Jr., *Phys. Chem. Chem. Phys.*, 2010
DOI: 10.1039/b924951f

Structural diversity of dimers of the Alzheimer Amyloid-(25-35) peptide and polymorphism of the resulting fibrils
Joan-Emma Shea, Andrew I. Jewett, Guanghong Wei, *Phys. Chem. Chem. Phys.*, 2010
DOI: 10.1039/c000755m

Guanine–aspartic acid interactions probed with IR–UV resonance spectroscopy†

Bridgit O. Crews,[a] Ali Abo-Riziq,[a] Kristýna Pluháčková,[b] Patrina Thompson,[c] Glake Hill,[c] Pavel Hobza[bd] and Mattanjah S. de Vries*[a]

Received 1st December 2009, Accepted 26th February 2010
First published as an Advance Article on the web 8th March 2010
DOI: 10.1039/b925340h

Double resonance spectroscopy of clusters of guanine with aspartic acid reveals geometries similar to patterns exhibited in DNA base pairs. In the spectral region of 32 800 cm^{-1} to 35 500 cm^{-1} we observe five isomers of guanine–aspartic acid clusters and assign their structures based on IR–UV hole-burning spectra and wave function theory calculations at the MP2/cc-pVDZ and MP2/cc-pVTZ levels. The calculations employed both harmonic and one-dimensional scan anharmonic approximations. Three of the isomers are similar, assigned to structures containing three hydrogen bonds and 9-enolguanine. We assign the fourth isomer to a structure containing a 9-keto tautomer of guanine and forming a triply bonded structure similar to a base pairing interaction. The fifth isomer dissociates with proton transfer upon excitation or ionization. This is the first set of experiments and high-level *ab initio* calculations of the isolated, microscopic interactions of an amino acid and a nucleobase, the building blocks of nucleic acids and proteins.

Introduction

The details of the interactions between proteins and DNA and the resulting recognition mechanisms are not understood in detail at the molecular level. The non-covalent forces that appear to govern such interactions are weak, and yet binding to certain sequences can be very specific. In fact, binding to specific sites can sometimes be orders of magnitude stronger than binding to random sites. The interaction between proteins and RNA is even more complex and less well understood because of the many structural motifs that RNA can adopt. Recognition can employ a combination of "direct readout"—involving functional groups, exposed in the major groove—or "indirect readout" influenced by structural differences between sequences.[1–3]

Although the complex of guanine with aspartic acid (Asp) might seem to be small or artificial in fact it is a real model system of interactions between a base pair and an amino acid. Both guanine and aspartic acid can be part of much larger system but still remain in the same structural complex with each other. We have found isomers in which aspartic acid binds to the Watson–Crick edge of guanine while the terminal COOH and NH_2 groups of aspartic acid remain available to form peptide bonds with other amino acids. This is possible because only the C═O part of the C-terminus COOH group participates in hydrogen bonding to guanine while the most important binding group appears to be the COOH group in the side-chain. In the protein data bank (www.pdb.org) there are 2318 structures containing a protein and a nucleic acid. Among these there are 208 contacts between guanine and aspartic acid within 3 Å. 47.1% of these contacts are between aspartic acid and phosphate groups; in 34.6% cases Asp is bound to the Watson–Crick edge of guanine, 11.5% of the Asp is in contact with a sugar, 5.3% of Asp are bound to the sugar edge of guanine, 1% to the Hoogsteen edge of guanine and 0.5% are in a stacked orientation with guanine.

When calculating frequencies, the complex of guanine with aspartic acid needs to be treated in an anharmonic way because as we have found for guanine,[4] distinguishing among the tautomers is impossible with the harmonic approximation. The same is true for the guanine–cytosine base pair where the three hydrogen bonds exhibit strongly anharmonic character.[5] Generally, rotational spectroscopic techniques provide spectra that are very difficult to unravel for larger systems and vibrational spectroscopic techniques do not usually provide enough structural information. Problems arise from nonlinear dependence of the complexity of the molecular dynamical problems on the number of actual vibrational degrees of freedom and from conformational complexity. A popular way of overcoming these problems is empirical scaling of the calculated harmonic frequencies. However, in the case of vibrational motions opposed by strongly anharmonic potentials (motions involved in hydrogen bonding) the approach is no longer reliable.[6] A possible solution is an adiabatic separation of the probing molecular modes. Being only few dimensional the resulting dynamical problems are tractable in a numerically exact way for practically any shape of the corresponding effective potentials.[7]

[a] *Department of Chemistry and Biochemistry, University of California Santa Barbara, CA 93106-9510, USA. E-mail: devries@chem.ucsb.edu*
[b] *Institute of Organic Chemistry and Biochemistry, Academy of Sciences of the Czech Republic and Center for Biomolecules and Complex Molecular Systems, Flemingovo nam. 2, 160 10 Prague 6, Czech Republic*
[c] *Department of Chemistry, Jackson State University, Jackson MS 39217-0510, USA*
[d] *Department of Physical Chemistry, Palacky University, 771 46 Olomouc, Czech Republic*
† Electronic supplementary information (ESI) available: Fig. S1–S3. See DOI: 10.1039/b925340h

Our current observations suggest that molecules other than nucleobases, such as amino acids, may also affect the excited state potential energy surface of the guanine nucleobase by clustering in geometries very similar to the geometry exhibited in base pairing. The fact that amino acids form complexes with guanine in base pair like structural motifs also highlights the idea that these interactions may serve to distinguish among bases in protein–nucleic acid interactions.[2,8]

Experimental method

The experimental set-up is described in detail elsewhere.[9] We laser desorb a mixture of pure compound from a graphite substrate with a Nd:YAG laser (1064 nm, $\sim$10 ns pulse duration, less than 1 mJ/pulse), after which the molecules become entrained into a pulsed supersonic jet of argon (backing pressure 6 atm). Using mass-selected spectroscopy we measure resonant two-photon ionization spectra (R2PI) by detecting positive ions in a reflectron time-of-flight mass spectrometer. In UV–UV double resonance experiments, two laser pulses are separated in time by 200 ns. Ionization laser intensities are approximately 3 mJ/pulse and are attenuated to avoid saturation. The first pulse serves as a ''burn'' pulse, which removes ground state population and causes depletion in the ion signal of the second ''probe'' pulse provided both lasers are tuned to a resonance of the same isomer. In IR–UV double resonance spectra the burn laser operates in the near-IR region. IR frequencies ranging from 3100 cm^{-1} to 3800 cm^{-1} are produced in an OPO setup (LaserVision) pumped by a Nd:YAG laser operating at its fundamental frequency.[10,11] Typical IR intensities in the burn region are 8–10 mJ $pulse^{-1}$ with a bandwidth of 3 cm^{-1}. The resulting ion-dip spectra are ground-state IR spectra that are optically selected by means of the probe laser R2PI wavelength and mass selected by virtue of the mass spectrometer detection.

Theoretical method

We model candidate structures for higher level calculations using the AMBER force field and perform simulated annealing as implemented in the Amber 7 program suite.[12,13] To create isolated gas-phase aspartic acid we started with a non-hydrogen bound form of aspartic acid, then modified the default zwitterionic amino and carboxylic termini to their neutral (gas-phase) forms, and generated new charges using antechamber.

For the naming of the clusters we have tried to remain consistent with that previously published on the structure of the isolated nucleobase guanine.[14] Keto clusters refer to any cluster in which guanine is in its 'keto' form, identified by a keto oxygen on carbon ''6'' of the purine ring structure. Enol structures refer to clusters in which guanine is in its 'enol' form, identified by an hydroxyl group on carbon ''6'' of the purine ring structure, and 'oxo-imino' forms are identified by a keto oxygen on carbon ''6'' of the purine ring structure combined with an imino nitrogen group on carbon ''2'' of the purine ring structure. The number which precedes the keto, enol, or oxo-imino refers to the placement of the mobile protons which attach to different atoms of the purine ring structure to form the multiple tautomers of guanine. The clusters we describe in most detail in the following discussion involve the 7,9-keto and 7,9-enol tautomers of guanine. These are clusters in which guanine is in the keto or enol form and a mobile proton is attached to either nitrogen ''7'' or nitrogen ''9'' of the purine ring structure.

We ran clusters of guanine–aspartic acid with guanine in each of its five lowest energy forms: 7, 9-keto, 7, 9-enol and 7-oxo-imino. We performed simulated annealing by running at a high temperature (800 K) for 30 ps followed by 10 ps of stepwise cooling and energy minimization. We imposed a distance restraint between guanine and aspartic acid during simulated annealing and removed it during energy minimization. The location of the restraint was varied in three rounds of annealing with 500 iterations of heating and stepwise cooling. We sorted the resulting structures according to energy, then optimized and calculated theoretical harmonic frequencies for unique structures. The resulting structures were re-optimized using B3LYP/6-31G to weed out high energy structures and minimize the number of structures to be calculated at a higher basis set; however, we found that guanine tautomerizes from enol to keto forms in this basis. When we ran identical structures in the 6-31+G* basis set, the enol forms did not tautomerize into the keto forms. We calculated B3LYP/6-31+G* energies and harmonic frequencies for approximately 30 clusters of each tautomer of guanine.

Because the calculation of the spectra must be done with the best possible geometries and most accurate method for comparison with the experimental data we re-optimized the lowest energy B3LYP structures by means of the MP2/cc-pVTZ method.[15,16] According to our previous experience this is the most suitable approach for hydrogen bonded as well as for stacked complexes of this size. We used the resolution of identity approximation for all MP2 calculations.[17] Each MP2/cc-pVTZ structure was then re-optimized using the MP2/cc-pVDZ method with tough convergence criteria (TURBOMOLE convergence criteria were set as scfconv $<1e^{-8}$, denconv $<1e^{-8}$ and gcart = 4) so that the structures were optimally minimized and frequency analysis could be done at the same level of theory. In addition to calculating interaction energies and interaction enthalpies at MP2/cc-pVDZ and MP2/cc-pVTZ levels we also included unscaled zero-point vibration energies (ZPVE) at the cc-pVDZ level of theory from harmonic vibrational frequency calculations and evaluated interaction and relative interaction enthalpies at both levels of theory.

For calculation of harmonic vibrational frequencies and IR spectra we used method NumForce as implemented in the TURBOMOLE 5.8 package program.[18] This method is based on knowledge of the molecular Hessian, matrix of second derivatives of total energies. Because very fast tautomerization processes exist in the complex we were interested in the anharmonicity of the individual vibrational modes. Therefore we also calculated one-dimensional anharmonic Hamiltonians and potential energy functions evaluated by means of the MP2/cc-PVDZ method. A typical stretch grid was constructed in the following way: hydrogen bonds were shortened by up to 0.25 Å with 0.025 Å steps and elongated by 1 Å with 0.05 Å steps up to 2 Å. This approach allowed good sampling of the

potential in all regions and smoothing by fitting to polynomials expressed in terms of the Morse variable y.

$$y = 1 - e^{-a(R-Re)}$$

Here a is a free parameter and R and Re are the actual and equilibrium bond length, respectively.

The methodology for assigning spectra was as follows. First we calculated unscaled MP2/cc-pVDZ infrared spectra using a harmonic approximation for all complexes, for keto and enol forms of guanine and for normal and protonated aspartic acid. Next we calculated one-dimensional potential energy scans of relevant hydrogens for protonated aspartic acid and for the most stable complexes in each of four structural groups: two keto and two enol complexes, each time one being triply and one doubly hydrogen bonded. After fitting these scans we obtained both harmonic and anharmonic frequencies of these vibrations. By comparing harmonic frequencies from one-dimensional scans and standard harmonic spectra we concluded how much each individual mode is coupled with other modes in the molecule. After comparing the harmonic and anhamormonic frequencies we obtained the amount of anharmonicity in each mode and calculated suitable scaling factors for each vibration. These we then applied to standard harmonic spectra. The resulting spectra therefore account for both anharmonicity and mode coupling. The intensities were taken directly from standard harmonic spectra because they are not as strongly influenced by anharmonicity as the vibrational frequencies themselves. Finally the spectra were compared to the experimental ones and if needed shifted by a constant to minimize the differences.

Results and discussion

Calculated structures

Fig. 1 shows the lowest energy structures found at the MP2/cc-pVTZ level for the clusters involving 9-keto and 9-enol tautomers of guanine. The calculations at B3LYP/6-31+G* level predicted a very similar set of structures for the clusters with 7-keto and 7-enol tautomers; however, in every case 7-keto containing structures are 2–3 kcal mol^{-1} higher in energy than their analogous 9-keto counterparts with virtually indistinguishable theoretical IR, the 7-enol tautomers being even higher in energy than 7-keto tautomers. For these reasons we show the structures and theoretical IR only for 9-keto structures. The B3LYP calculations also predict that clusters containing oxo-imino tautomers of guanine are more than 8 kcal mol^{-1} higher in energy than clusters containing keto tautomers. Additionally, IR frequencies of clusters involving oxo-imino tautomers do not match any of the experimental IR spectra.

The structures in Fig. 1 are labeled according to tautomeric form and relative energy calculated at the B3LYP/6-31+G* level. 9E1 is the lowest energy cluster found with guanine in 9-enol form, 9K2 is the second lowest energy cluster found for guanine in 9-keto form, *etc*. Structures 9EN and 9KN were not predicted by B3LYP/6-31+G* to be in the set of the most stable structures but they appeared after re-optimization at the MP2/cc-pVTZ level of theory, whereby the 9KN structure emerged as the global minimum. Relative interaction electronic energies and enthalpies (in parentheses) are given in kcal mol^{-1} and are relative to the lowest energy cluster we found, 9KN. The lowest energy structure contains 9-keto guanine in a 'base pairing' type configuration in which aspartic acid binds to the base pairing site of guanine through three hydrogen bonds. 9K1 and 9K5 have a similar type of interaction, slightly higher in energy by 1.88 and 2.40 kcal mol^{-1}, respectively. The 9-enol guanine structures 9EN and 9E7 are analogous but higher in energy by 4.93 and 4.60 kcal mol^{-1}, respectively. Structure 9E1 exhibits a bifurcated hydrogen bond between both oxygens of the COOH group of aspartic acid and hydrogen in the NH_2 group of guanine. This structure is only 2.56 kcal mol^{-1} higher in energy than the most stable structure, 9KN. However, this binding motif is quite unique for the isolated molecules because when aspartic acid is part of a protein the COOH group is part of a peptide bond and it is likely that this type of interaction cannot occur. Complexes with two H-bonds are less stable than complexes with three H-bonds and the 9-keto complexes generally are lower in energy than 9-enol complexes. Structure 9K6 is shown for comparison as it presents the only structure where aspartic acid is bonded to the sugar edge of guanine. However this complex has only two H-bonds and is 11.04 kcal mol^{-1} higher in energy. All of the clusters involve hydrogen bonds with the side-chain of aspartic acid.

UV spectra

Fig. 2 shows the mass spectrum and the R2PI spectrum from 32 800 cm^{-1} to 33 900 cm^{-1}. Upon scanning to 35 500 cm^{-1} we observed no additional peaks. We performed UV–UV double resonance spectroscopy to determine that the R2PI spectrum consists of four isomers. The origins of these isomers are labeled I–IV in Fig. 2. The R2PI spectrum of isomer I is much broader than those of isomers II–IV and red-shifted by almost 1000 cm^{-1} relative to isomers II–IV. Because the R2PI spectrum of isomer I is broad, without the sharp peaks exhibited by isomers II–IV, we cannot exclude that this part of the spectrum consists of overlapping contributions from more than one isomer, as will be discussed below.

We also observe a peak for protonated aspartic acid in the mass spectrum. Since aspartic acid does not absorb at any of the UV wavelengths in these experiments, the only possibility is that this peak arises from an excited or ionized guanine–aspartic acid cluster that undergoes proton transfer and dissociation to form protonated aspartic acid. This cluster corresponds to isomer V as determined by double resonance spectroscopy, described below.

IR spectra

Figs. 3 and 4 show the experimental IR–UV hole-burning spectra in comparison with calculated anharmonic frequencies, displayed as stick spectra. In both figures the calculated spectra are ordered from top to bottom according to increasing relative energy of their respective structures. The relative calculated intensities appear in Table 1. Fig. 3 shows the experimental data for isomer I together with the calculated frequencies for the keto structures, while Fig. 4 shows the data for isomers

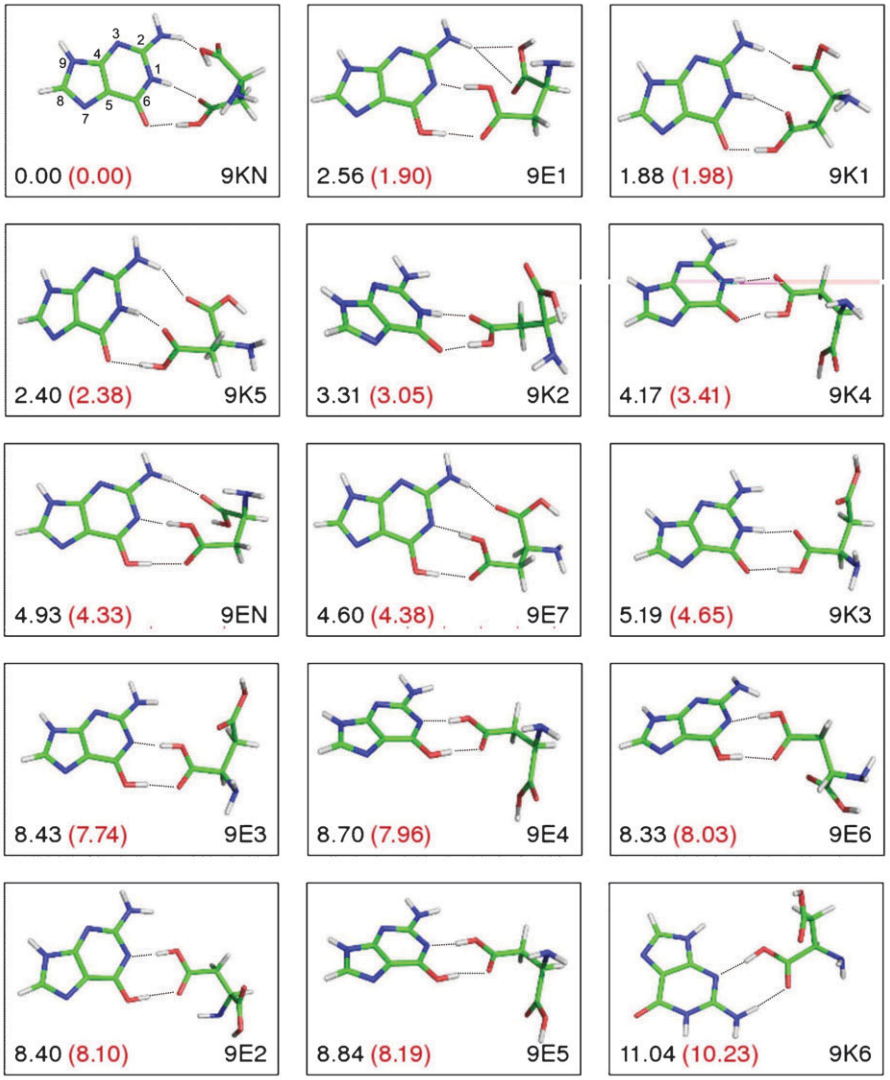

Fig. 1 Lowest energy structures of 9-keto and 9-enol guanine–aspartic acid clusters calculated at MP2/cc-pVTZ level. Both relative interaction energies in black and relative interaction enthalpies in red in parenthesis are BSSE corrected and in kcal mol^{-1}. All energies are relative to structure 9KN.

II–IV and the calculated enol frequencies. The stick spectra are color coded to show the vibrational modes corresponding to colors in the structures in the insets as follows. Guanine modes: red- $N9H_{free}$, yellow- $N3H_{HB}$ for the keto and OH_{HB} for the enol form, orange- $NH2_{HB}$ symmetrical stretch, purple- $NH2_{free}$ antisymmetric stretch. Aspartic acid modes: blue- $COOH_{R-group,HB}$, green- $COOH_{C\text{-}terminus}$, light blue- NH_2 symmetric stretch, grey- NH_2 antisymmetric stretch.

The IR spectra of isomers II–IV are very similar, while that of isomer I is distinctly different. This observation strongly suggests that isomers II–IV are variations of similar cluster structures, possibly differing only by small changes in amino acid conformation or by 7H *versus* 9H tautomer form. The latter explanation is less likely taking into consideration the large shift between electronic origins of the 7H enol and 9H enol forms of free guanine which are shifted by more than 1600 cm^{-1} relative to each other.[19–21] Isomer I on the other hand exhibits a significantly different IR spectrum, suggesting that it belongs to a very different cluster structure. The four lowest energy calculated structures belong to two families: triply hydrogen bonded structures with keto guanine (9Kx) *versus* triply hydrogen bonded structures with enol guanine (9Ex). Clusters which are only doubly bonded structures are at least 3 kcal mol^{-1} higher in energy. Therefore we propose that the two types of observed IR spectra (for isomer I *versus* isomers II–IV) represent those two families of structures. Comparison with the corresponding calculated frequencies provides a better fit for the enol structures for isomers II–IV and the keto structures for isomer I, as further detailed below.

Isomer I. Isomer I, which shows only two peaks above 3400 cm^{-1}, with possibly a shoulder red of the 3500 cm^{-1}, peak matches well with the low energy keto structures. These structures show three frequencies (N9H and the asymmetric NH_2 stretches for the guanine and the aspartic acid) which nearly coincide and could very well result in a single

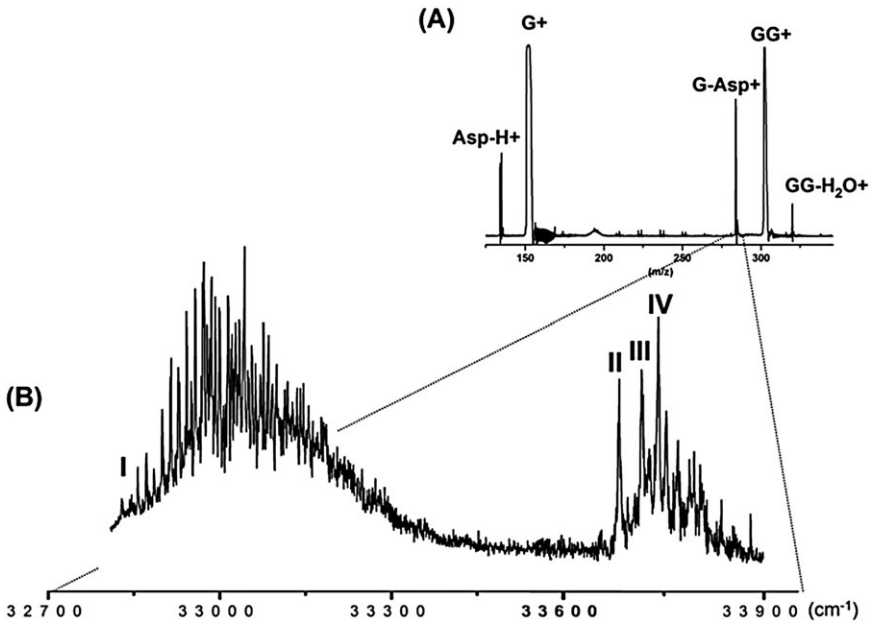

Fig. 2 (A) Mass spectrum of guanine–aspartic acid. (B) R2PI spectrum of guanine–aspartic acid with unique isomer origins labeled I–IV as revealed by UV–UV hole burning.

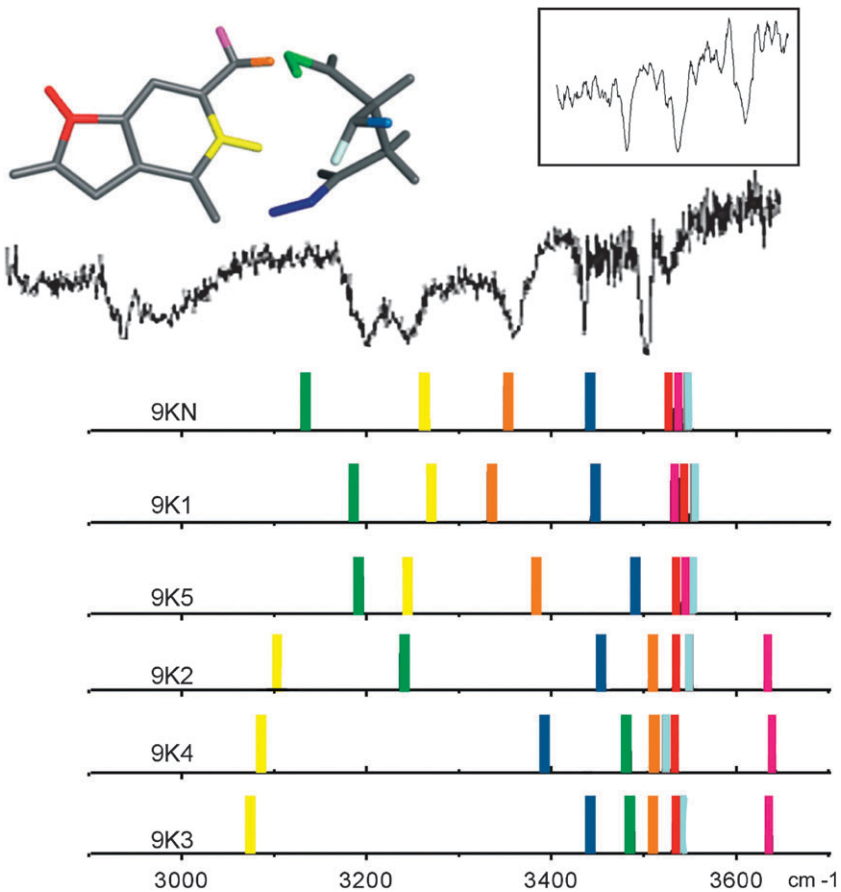

Fig. 3 IR hole-burning spectrum of isomer I. Stick spectra show anharmonic frequencies calculated for the lowest energy keto structures. See Table 1 for relative intensities. Color coding indicates modes as shown in the 9KN structure at the top and specified in the text. The spectrum in the inset is from protonated aspartic acid fragments, due to isomer V.

unresolved peak at about 3500 cm^{-1} or one with a shoulder, and the symmetric aspartic acid NH_2 peak at about 3400 cm^{-1}. The three broad peaks between 3200 and 3400 cm^{-1} are also well reproduced, especially for the lowest energy 9KN

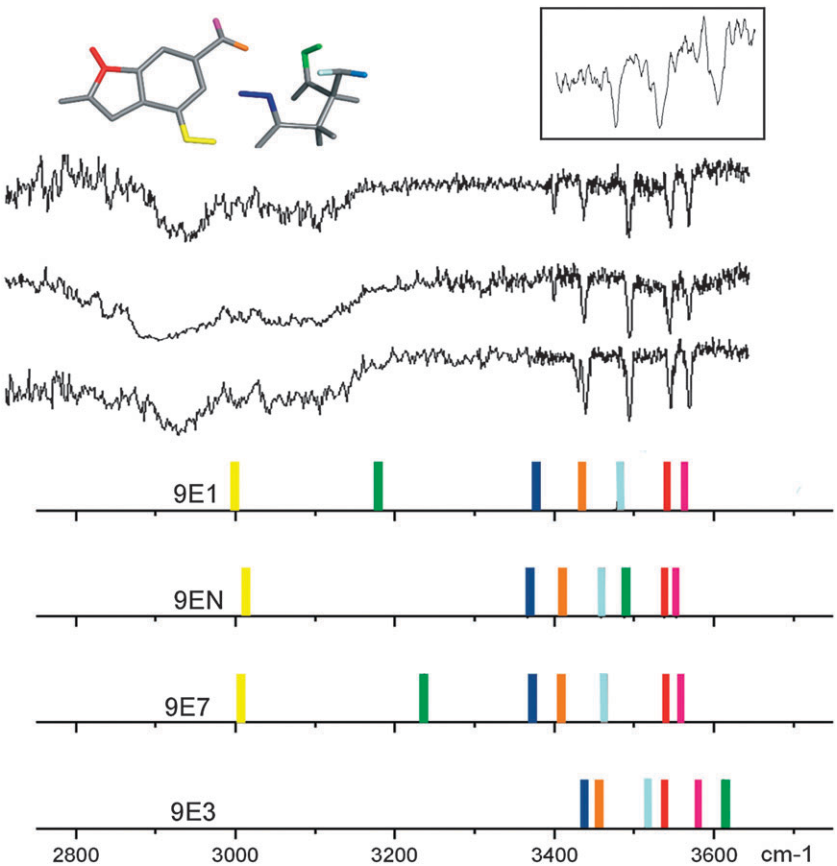

Fig. 4 IR hole-burning spectrum of isomers II–IV. Stick spectra show anharmonic frequencies calculated for the lowest energy enol structures. See Table 1 for relative intensities. Color coding indicates modes as shown in the 9EN structure at the top and specified in the text. The spectrum in the inset is from protonated aspartic acid fragments, due to isomer V.

structure. Once again the R group carbonyl would be red-shifted outside the experimental window. This leaves the broad peaks around 3000 cm^{-1} unassigned. One possibility is that this peak corresponds to the hydrogen bound COOH group of aspartic acid, which is predicted by harmonic approximation to be at 2833 cm^{-1}. As noted before it is quite possible that multiple related structures overlap in this UV region that cannot be separated by the probe laser due to the broad UV spectrum. Once again, the 7H analogous structures would produce similar IR signatures. They would be slightly higher in energy and, especially given the broad UV spectrum for this isomer (or family of isomers) they may be present as well.

Isomers II–IV. The IR spectra of isomers II–IV are characterized by five peaks in the range of 3400–3600 cm^{-1} with an additional two broad peaks between 2800 cm^{-1} and 3100 cm^{-1}. This pattern is very well reproduced by the enol structures, particularly two of the three lowest energy ones, 9E1 and 9E7. 9E3 shows an unlikely fit to the experimental data, both in absolute frequency and spacing. 9EN is similar but the C terminus OH mode is not shifted as much as in the other two cases, presumably because it is hydrogen bonding less with the N terminus. This OH mode interacts with the electron pair N-terminus nitrogen and this small hydrogen bonding interaction modifies both the OH and the NH_2 frequencies involved. The three lowest energy enol structures differ mostly in the conformation of the C terminus which would be expressed in subtle shifts in the frequencies of those two modes. The top two experimental traces in Fig. 4 are very similar while the NH_2 is slightly blue-shifted in the bottom trace. In all enol structures the R group carbonyl, where the R group corresponds to the side-chain of aspartic acid, is engaged in strong hydrogen bonding with the guanine and red-shifted to below 2000 cm^{-1}, outside the experimental range. The 7H analogous structures would be slightly higher in energy and would produce essentially the same IR signatures, however by analogy with the monomer guanine spectrum we would expect them to be significantly shifted in the UV. If this analysis is correct they may still remain to be observed at a different UV wavelength range.

Isomer V. Fig. 3 and 4 show in an inset at the top the IR–UV hole-burning spectrum measured at the mass of protonated aspartic acid (Asp-H+). Since this species does not absorb in the given UV range it has to be a cluster fragment, formed either in the excited state or in the ionic state. Therefore this IR spectrum must belong to the originating cluster. Since additional free IR bands would appear in the IR spectrum if Asp-H^+ originated from a more complex cluster, it is unlikely that this peak originates from a higher order cluster, such as guanine dimer–aspartic acid, and therefore it is likely that it is a dissociation product of G-Asp clusters. This portion of the

Table 1

	Hessian		Scan
9E3	Harmonic freq.	Intensities	Anharmonic freq.
COOH HB Asp	2787.2	2787.26	—
COOH Asp C-term Asp	3761.3	73.53	3611.606
OH HB G	3273.3	3273.32	—
NH2s HB G	3589.3	58.33	3454.726
N9H G	3674	106.03	3537.703
NH2a HB G	3718	52.76	3580.936
NH2s Asp	3511.8	3.81	3438.052
NH2a Asp	3594.8	8.49	3519.309
9E7	Harmonic freq.	Intensities	Anharmonic freq.
NH2s HB G	3545	326.92	3408.014
NH2a HB G	3693	118.79	3556.857
N9H G	3675	104.9	3538.778
COOH Asp C-term	3484	359.67	3237.038
OH HB G	3323	1930.7	3006.189
COOH HB	2668	2898.07	1812.5
NH2a Asp	3616	9.4	3460.512
NH2s Asp	3523	11.97	3371.511
9EN	Harmonic freq.	Intensities	Anharmonic freq.
NH2s HB G	3546	287.64	3408.975
NH2a HB G	3689	130.51	3553.005
N9H G	3674	95.41	3537.815
COOH Asp C-term	3754	77.68	3487.899
OH HB G	3331	1792.91	3013.426
COOH HB	2681	2851.97	1821.332
NH2a Asp	3614	23.05	3458.598
NH2s Asp	3517	12.5	3365.769
9E1	Harmonic freq.	Intensities	Anharmonic freq.
NH2s HB G	3574	160.27	3435.893
NH2a HB G	3702	93.49	3565.525
N9H G	3675	107.08	3538.778
COOH Asp C-term	3421	380.19	3178.504
OH HB G	3316	1973.38	2999.856
COOH HB	2435	3697.09	1654.212
NH2a Asp	3635	24.6	3478.695
NH2s Asp	3532	12.92	3380.124
	Hessian		
9KN	Harmonic freq.	Intensities	Anharmonic freq.
COOH HB	2833	2413.18	2310.878
COOH Asp C-term	3382	348.31	3134.267
N3H HB G	3422	678.44	3262.743
NH2s HB G	3511	403.24	3353.303
N9H G	3671	96.54	3534.815
NH2a HB G	3674	122	3537.256
NH2s Asp	3515	30.29	3441.185
NH2a Asp	3624	34.82	3547.896
9K1			
COOH HB	2881	2281.48	2350.032
COOH Asp C-term	3437	580.14	3185.239
N3H HB G	3427	491.81	3267.511
NH2s HB G	3491	588.66	3334.201
N9H G	3675	116.12	3538.666
NH2a HB G	3671	93.74	3534.367
NH2s Asp	3521	11.49	3447.059
NH2a Asp	3627	18.21	3550.833
9K5			
COOH HB	2948	2220.38	2404.684
COOH Asp C-term	3444	418.54	3191.726
N3H HB G	3402	855.5	3243.674
NH2s HB G	3543	294.76	3383.865
N9H G	3672	103.73	3535.777
NH2a HB G	3682	128.47	3544.958
NH2s Asp	3520	0.79	3446.08
NH2a Asp	3621	12.26	3544.959
	Hessian		
9K2	Harmonic freq.	Intensities	Anharmonic freq.
COOH HB	2869	2690.82	2340.243
COOH Asp C-term	3497	250	3240.844
N3H HB G	3256	1878.95	3104.469
NH2s HB G	3584	71.58	3508.736
N9H G	3671	103.62	3534.815

Table 1 (*continued*)

	Hessian		Scan
NH2a HB G	3712	60.93	3634.048
NH2s Asp	3530	38.21	3455.87
NH2a Asp	3628	29.62	3551.812
9K3			
COOH HB	2989	1949.07	2438.127
COOH Asp C-term	3762	72	3486.432
N3H HB G	3224	2349.25	3073.958
NH2s HB G	3585	67.32	3509.715
N9H G	3671	103.3	3534.815
NH2a HB G	3714	57.53	3636.006
NH2s Asp	3517	4.16	3443.143
NH2a Asp	3610	7.98	3534.19
9K4			
COOH HB	2915	2491.1	2377.766
COOH Asp C-term	3757	71.71	3481.799
N3H HB G	3237	2111.26	3086.353
NH2s HB G	3587	69.52	3511.673
N9H G	3671	104.93	3534.815
NH2a HB G	3717	60.8	3638.943
NH2s Asp	3513	3.98	3439.227
NH2a Asp	3601	10.21	3525.379

IR spectrum does not match any of the other IR spectra so we conclude that the parent cluster must be a different isomer. Unfortunately the signal-to-noise ratio did not permit measurement of a larger range of the spectrum or of a well-resolved UV spectrum. Since spectral assignment on the basis of three peaks is tenuous at best, identification of this fifth, UV unstable, isomer must await additional data.

Fig. S3 of the ESI† shows one-dimensional potential hydrogen scans of five hydrogens ($COOH_{HB,Asp}$, $COOH_{Asp–C\ terminus}$, $N9H_G$, $N3H_{HB,G}$ and $NH_{2–s,HB,G}$). The colors of individual curves correspond to those in Fig. 3. The hydrogens involved in hydrogen bonds exhibit strongly anharmonic behavior and cannot be correctly described by harmonic potentials. The calculated spectra in Fig. 3 and 4 include the anharmonic correction. An even more complete correction would require two-dimensional scans for the NH_2 group as well as inclusion of the movement of heavy atoms along the hydrogen bond coordinate.

Energetics alone are not enough to make an assignment, as previously demonstrated by the lack of observation of the lowest energy guanine monomers in R2PI experiments.[22] We do note an intriguing similarity between the origins of the R2PI spectra of isomer I and the guanine–cytosine base pair, suggesting that the electronic configuration of guanine is similar in these two clusters, which we expect if the structure and bonding pattern of guanine is very similar in the two clusters. This observation, illustrated in Fig. 5, suggests that guanine in isomer I has a similar electronic configuration and structure to that of guanine in the Watson–Crick base pair which originates from a keto tautomer, and is simulated by 9-substituted guanine and 1-substituted cytosine in place of the DNA backbone.[23,24] The spectra are similar in the frequencies of their electronic origins. The R2PI spectra of both guanine–aspartic acid and guanine–cytosine base pairs begin near 32 800 cm^{-1} and continue as broad spectra for several hundred wavenumbers. Guanine–aspartic acid isomers II–IV, which are assigned as 9-enol containing tautomers and 9-enol guanine monomer have electronic origins far blue-shifted, near 33 700 cm^{-1} and 34 800 cm^{-1}, respectively. The guanine dimer is also suspected to contain 9-keto guanine in a similar base pairing configuration. Its R2PI spectrum is slightly less red-shifted and not as broad; however, a lower energy symmetric structure has, so far, not been observed in the gas phase, presumably due to a short excited state lifetime.

Conclusion

UV and IR double-resonance spectra in the region 32 800 cm^{-1} to 35 500 cm^{-1} reveal five isomers of guanine–aspartic acid. Guanine–aspartic acid isomer I contains three hydrogen bonds and involves the 9-keto tautomer of guanine. The binding motif in this complex is similar to a Watson–Crick motif seen in the guanine–cytosine base pair. The UV spectrum of this isomer is broad and it is possible that it consists of overlapping spectra of a family of overlapping and very similar structures. These additional structures could involve subtle differences in amino acid conformations or 7H guanine tautomers. Three of the isomers (II–IV) fit calculated structures with two hydrogen bonds between a 9-enol tautomer of guanine and aspartic acid. While 9-keto guanine is not observed in R2PI experiments on guanine monomers, the electronic origin of guanine–aspartic acid isomer I is red-shifted approximately 1000 cm^{-1} relative to the three 9-enol clusters and is near the electronic origin of previously measured 9-keto containing guanine clusters including the Watson–Crick guanine–cytosine base pair suggesting that this specific bonding geometry makes it possible to observe the keto form of guanine whereas under identical conditions free guanine is unobservable as a keto form likely due to a shortened excited state lifetime. A fifth isomer is observed but not assigned, as it appears as protonated aspartic acid fragments. This is the first set of experiments and high level *ab initio* calculations of the isolated, microscopic interactions of an amino acid and a nucleobase, the building blocks of nucleic acids and proteins.

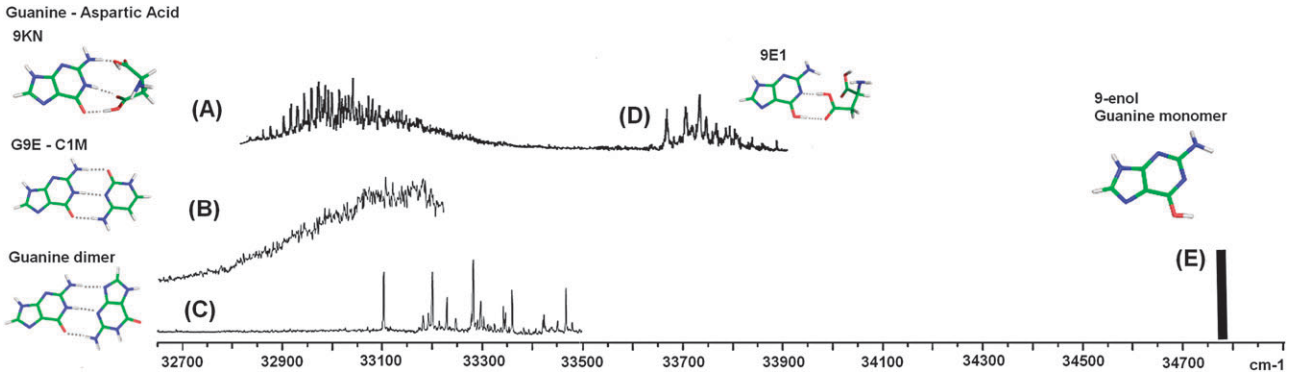

Fig. 5 R2PI spectra of guanine–aspartic acid structure 9KN (A), guanine-9-ethyl-cytosine-1-methyl, forming the Watson–Crick base pair (B), the guanine dimer (C), guanine–aspartic acid structure 9E1 (D) and 9-enol guanine monomer (E).

Acknowledgements

This work was supported by the Ministry of Education, Youth and Sports of the Czech Republic (Grants No. LC512 and MSM 6198959216) and by the Grant Agency of the Academy of Sciences of the Czech Republic (A400550510); it was also part of the research project No. Z4 055 0506. The support of the Praemium Academiae of the Academy of Sciences of the Czech Republic, awarded to P. H. in 2007, is also acknowledged. The experimental work was supported by the National Science Foundation under CHE-0911564.

References

1 P. A. Rice and C. C. Corell, *Protein–Nucleic Acid Interactions*, Royal Society of Chemistry, Cambridge, 2008.
2 N. C. Seeman, J. M. Rosenberg and A. Rich, *Proc. Natl. Acad. Sci. U. S. A.*, 1976, **73**, 804.
3 J. L. Battiste, M. Hongyuan, N. Sambasiva Rao, T. Ruoying, D. R. Muhandiram, L. E. Kay, A. D. Frankel and J. R. Williamson, *Science*, 1996, **273**, 1547.
4 D. Nachtigallová, P. Hobza and V. Špirko, *J. Phys. Chem. A*, 2008, **112**, 1854.
5 B. Brauer, R. B. Gerber, M. Kabelac, P. Hobza, J. M. Bakker, A. G. A. Riziq and M. S. de Vries, *J. Phys. Chem. A*, 2005, **109**, 6974.
6 K. Giese, M. Petković, H. Naundorf and O. Kühn, *Phys. Rep.*, 2006, **430**, 211.
7 W. P. Kraemer, V. Spirko and O. Bludsky, *J. Mol. Spectrosc.*, 1994, **164**, 500.
8 A. C. Cheng and A. D. Frankel, *J. Am. Chem. Soc.*, 2004, **126**, 434.
9 G. Meijer, M. S. de Vries, H. E. Hunziker and H. R. Wendt, *Appl. Phys. B: Photophys. Laser Chem.*, 1990, **51**, 395.
10 R. N. Pribble, A. W. Garrett, K. Haber and T. S. Zwier, *J. Chem. Phys.*, 1995, **103**, 531.
11 M. Schmitt, H. Muller and K. Kleinermanns, *Chem. Phys. Lett.*, 1994, **218**, 246.
12 D. A. Case, T. E. Cheatham, T. Darden, H. Gohlke, R. Luo, K. M. Merz, A. Onufriev, C. Simmerling, B. Wang and R. J. Woods, *J. Comput. Chem.*, 2005, **26**, 1668.
13 D. A. Case, D. A. Pearlman, J. W. Caldwell, T. E. Cheatham, W. S. Ross, C. L. Simmerling, T. A. Darden, K. M. Merz, R. Stanton, A. L. Cheng, J. J. Vincent, M. Crowley, V. Tsui, H. Gohlke, R. J. Radmer, Y. Duan, J. Pitera, I. Massova, G. L. Siebel, U. C. Singh and P. K. Weiner, *AMBER*, 7th edn, University of California, 2002.
14 M. Mons, F. Piuzzi, I. Dimicoli, L. Gorb and J. Leszczynski, *J. Phys. Chem. A*, 2006, **110**, 10921.
15 C. Møller and M. S. Plesset, *Phys. Rev.*, 1934, **46**, 618.
16 R. A. Kendall, T. H. Dunning and R. J. Harrison, *J. Chem. Phys.*, 1992, **96**, 6796.
17 M. Feyereisen, G. Fitzgerald and A. Komornicki, *Chem. Phys. Lett.*, 1993, **208**, 359.
18 R. Ahlrichs, M. Bar, M. Haser, H. Horn and C. Kolmel, *Chem. Phys. Lett.*, 1989, **162**, 165.
19 W. Chin, M. Mons, I. Dimicoli, F. Piuzzi, B. Tardivel and M. Elhanine, *Eur. Phys. J. D*, 2002, **20**, 347.
20 M. Mons, I. Dimicoli, F. Piuzzi, B. Tardivel and M. Elhanine, *J. Phys. Chem. A*, 2002, **106**, 5088.
21 E. Nir, C. Janzen, P. Imhof, K. Kleinermanns and M. S. de Vries, *J. Chem. Phys.*, 2001, **115**, 4604.
22 K. Seefeld, R. Brause, T. Haber and K. Kleinermanns, *J. Phys. Chem. A*, 2007, **111**, 6217.
23 A. Abo-Riziq, B. Crews, L. Grace and M. S. de Vries, *J. Am. Chem. Soc.*, 2005, **127**, 2374.
24 A. Abo-Riziq, L. Grace, E. Nir, M. Kabelac, P. Hobza and M. S. de Vries, *Proc. Natl. Acad. Sci. U. S. A.*, 2005, **102**, 20.